

The local structure of protonated water from x-ray absorption and density functional theory

Matteo CavalleriLars-Åke NäslundDavid C. EdwardsPhilippe WernethHirohito OgasawaraSatish MyneniLars OjamäeMichael OdeliusAnders NilssonLars G. M. Pettersson

Citation: *The Journal of Chemical Physics* **124**, 194508 (2006); doi: 10.1063/1.2199828

View online: <http://dx.doi.org/10.1063/1.2199828>

View Table of Contents: <http://aip.scitation.org/toc/jcp/124/19>

Published by the *American Institute of Physics*

COMPLETELY

REDESIGNED!



**PHYSICS
TODAY**

Physics Today Buyer's Guide
Search with a purpose.

The local structure of protonated water from x-ray absorption and density functional theory

Matteo Cavalleri

Fysikum, AlbaNova University Center, Stockholm University, SE-106 91 Stockholm, Sweden

Lars-Åke Näslund

Fysikum, AlbaNova University Center, Stockholm University, SE-106 91 Stockholm, Sweden and Stanford Synchrotron Radiation Laboratory, P.O. Box 20450, Stanford, California 94309

David C. Edwards

Department of Chemistry, Princeton University, Princeton, New Jersey 08544

Philippe Wernet

Stanford Synchrotron Radiation Laboratory, P.O. Box 20450, Stanford, California 94309 and BESSY, Albert-Einstein-Strasse 15, D-12489 Berlin, Germany

Hirohito Ogasawara

Stanford Synchrotron Radiation Laboratory, P.O. Box 20450, Stanford, California 94309

Satish Myneni

Department of Geosciences, Princeton University, Princeton, New Jersey 08544

Lars Ojamäe

Department of Chemistry, IFM, Linköping University, SE-581 83 Linköping, Sweden

Michael Odelius

Fysikum, AlbaNova University Center, Stockholm University, SE-106 91 Stockholm, Sweden

Anders Nilsson

Stanford Synchrotron Radiation Laboratory, P.O. Box 20450, Stanford, California 94309 and Fysikum, AlbaNova University Center, Stockholm University, SE-106 91 Stockholm, Sweden

Lars G. M. Pettersson^{a)}

Fysikum, AlbaNova University Center, Stockholm University, SE-106 91 Stockholm, Sweden

(Received 23 February 2006; accepted 4 April 2006; published online 18 May 2006)

We present a combined x-ray absorption spectroscopy/computational study of water in hydrochloric acid (HCl) solutions of varying concentration to address the structure and bonding of excess protons and their effect on the hydrogen bonding network in liquid water. Intensity variations and energy shifts indicate changes in the hydrogen bonding structure in water as well as the local structure of the protonated complex as a function of the concentration of protons. In particular, in highly acidic solutions we find a dominance of the Eigen form, H_3O^+ , while the proton is less localized to a specific water under less acidic conditions. © 2006 American Institute of Physics.

[DOI: [10.1063/1.2199828](https://doi.org/10.1063/1.2199828)]

I. INTRODUCTION

One of the most fundamental chemical processes in aqueous solutions is the acid-base reaction involving a solvated proton. The proton transport in aqueous media is anomalously fast and forms an integral part of nearly all biological and geochemical charge-transfer reactions as well as, e.g., charge transport in modern fuel cells. In spite of significant efforts, however, the detailed structure of the protonated water complex in terms of the limiting Zundel¹ (H_5O_2^+) and Eigen² (H_3O^+) structural motifs has remained elusive.

Conversion between the Zundel and Eigen forms has been proposed as part of the proton transport in water and

from theoretical simulations fluxional intermediate structures are indicated.³ A direct, experimental structure determination based on vibrational spectra of liquid water with excess protons is complicated because the spectra are broad and featureless. In spite of this a recent combined experimental and theoretical study indicated that both forms are present in a 1M solution of hydrochloric acid⁴ (HCl) while only the Eigen form was found in a recent analysis of neutron diffraction data from a concentrated HCl solution.⁵ In this context mass-selected protonated water clusters are of great current interest since they form a bridge between well-defined molecular structures and disordered liquid water. They provide strong structural information through their vibrational spectra as systematic changes between the Eigen and Zundel forms are observed in the size range of 2–11 water molecules as function of the symmetry of the clusters.⁶ However, the

^{a)}Fax: +46 (8)5537 8442. Electronic mail: lgm@physto.se

extension to bulk liquid water is nontrivial and a more direct, local experimental probe of the coordination in acidic solutions is desirable.

Recently, it has been reported that oxygen *K*-edge x-ray absorption spectroscopy (XAS) as well as x-ray Raman scattering (XRS) of pure liquid water^{7–9} are sensitive to the hydrogen (H)-bonded network. H-bonded O–H groups were found to give a signal at 540–541 eV (denoted postedge) while unsatisfied H bonds are indicated through intensities at 535 eV (pre edge) and 537–538 eV (main edge).⁸ In combination with density functional theory (DFT) spectrum calculations, XAS/XRS provides precisely the local probe needed to analyze the H-bonded network in the liquid.⁸

In the present work we extend our approach to a detailed analysis of the H bonding in protonated water as a function of the proton concentration. We observe spectral changes in both the preedge and postedge regions that are clearly different at low and high concentrations indicating significant changes in the nature of the protonated species and in the H-bonding network of surrounding water.

II. METHODS

A. Experimental technique

The O(*1s*) x-ray absorption (XA) spectra were collected on beamline 8.0 at the Advanced Light Source (ALS), Lawrence Berkeley National Laboratory, CA, USA. The liquid solutions were held under atmospheric pressure and room temperature in the Soft X-ray Endstation for Environmental Research (SXEER), which separates the helium-filled sample chamber from the vacuum in the synchrotron beamline. The XA spectra were measured indirectly via the fluorescence yield technique, which provides a reliable high-resolution absorption spectrum of bulk water.¹⁰ Further description of the experiment and data treatment can be found elsewhere.¹¹

The signal intensity I_f is proportional to the linear absorption coefficient, $\mu_x(h\nu)$, which is the aim of XAS. However, if the sampling depth of the yield technique is not significantly smaller than the x-ray penetration length, as in the case of fluorescence yield XAS of water, the proportionality is not linear.^{10–12} The symptoms of this nonlinearity are compressed spectral features and saturation of the XA spectrum. The saturated spectra, $I_f(h\nu)$, can in many cases be compensated to give $\mu_x(h\nu)$ through

$$\mu_x(h\nu) = C'(\varepsilon_f) \frac{I_f(h\nu)}{I_0} \left/ \left(1 - C''(\varepsilon_f) \frac{I_f(h\nu)}{I_0} \right) \right., \quad (1)$$

where I_0 is the incident photon flux density, $C'(\varepsilon_f)$ is a scaling factor, and $C''(\varepsilon_f)$ is the saturation compensating factor of the fluorescence with energy ε_f . Further details of the correction procedure are given elsewhere.¹¹ All XA spectra in the present work have been compensated for saturation effects.

B. Samples

Hydrochloric acid, HCl(aq), 37% in weight in water, was purchased from Sigma-Aldrich. The concentrated solution

was diluted using de-ionized water without any further preparations to give the concentrations 0.1, 1, 4, and 6M.

C. Theoretical details

The XA spectra were generated within a DFT framework using the STOBED-DEMON program¹³ with the gradient-corrected exchange and correlation functionals developed by Becke¹⁴ and Perdew,¹⁵ respectively. The core hole was simulated by applying Slater's transition-potential approach.^{16–18} This is obtained with the core orbital having half an electron removed, which represents a good balance between initial and final state effects in the case of water.¹⁹ The half-core-hole potential used in the DFT spectrum calculations has been critically evaluated by Cavalleri *et al.*¹⁹ and shown to be accurate and superior in the case of water to the alternative full-core-hole approach.²⁰

The core-excited oxygen was described using the IGLO-III all-electron basis set of Kutzelnigg *et al.*²¹ Effective core potentials²² (ECP), which eliminate the O(*1s*) level, were used on all oxygen atoms but the core-excited one in order to simplify the definition of the core hole. The hydrogen was described with the Huzinaga (*5s*) basis set extended with one *p* function and contracted to [*3s, 1p*].²³ The calculations were performed using a double-basis set technique where, in the spectrum calculation, the normal molecular basis was augmented by a large diffuse basis (≈ 150 functions) in order to improve the description of the Rydberg and continuum states.²⁴

An XA calculation results in a discrete set of energy levels, each associated with an oscillator strength and a line broadening. The experimental broadening of a transition depends on instrumental, lifetime, and vibrational effects, which can be mimicked by convoluting the obtained oscillator strengths in the theoretical spectra with Gaussians of linearly increasing full width at half maximum (FWHM). The method has been shown to give a reliable description of XA spectra for water in its condensed phases^{7,8,25,26} as well as for gas-phase molecules such as pyridine²⁷ and methanol.²⁵ The effects on the spectra from H-bond formation have been studied and compared with experiment for the ordered (3×2) overlayer of glycine on Cu(110)²⁸ as well as for bulk methanol.²⁹ We have furthermore shown that a fully periodic plane-wave calculation of the XA spectra using the Car-Parrinello molecular dynamics³⁰ (CPMD) approach is in complete agreement with the localized basis set cluster model calculation once the unit cell and cluster sizes are large enough.³¹

The total spectra from the molecular dynamics configurations were obtained by summing the spectra of all selected structures using a constant 0.5 eV broadening of all peaks; the variations in energy resulting from variations in structure provide an effective broadening of the higher peaks which results in smooth spectra also with this smaller broadening.

The use of a half-occupied core hole takes care of relaxation effects up to second order^{16,17} and reproduces the excitation energy of the core level to within 2 eV of the experimental value on the absolute energy scale. The final absolute energy scale is obtained with precision of the order of 0.5 eV

TABLE I. Optimized bond lengths and angles of the H_3O^+ and H_5O_2^+ clusters in this work. MP2 calculations described in Ref. 34.

| | Eigen H_3O^+ | Zundel H_5O_2^+ |
|--|------------------------------|---------------------------------|
| $R(\text{O}-\text{H})$ | 1.01 Å | 1.0 Å |
| $R(\text{O} \dots \text{H}^+)$ | 1.01 Å | 1.2 Å |
| $R_{\text{HB}}(\text{O} \dots \text{H})$ | 1.55 Å | 1.7 Å |
| $\angle(\text{O} \dots \text{H}^+ \dots \text{O})$ | 174.98 | 175.68 |

by correcting the spectral energy scale through the Δ Kohn-Sham approach proposed by Triguero *et al.*,^{18,27,32} where the XA spectrum is uniformly shifted by matching the lowest oscillator strength to the energy difference between the total Kohn-Sham energies of the first resonant core-excited and the ground state parent cluster.

Relativistic effects can be rather small but yet significant for core-ionization energies of the first-row elements, such that it is a good approximation to add these effects as a perturbation based on atomic calculations. The revised value of +0.33 eV for the relativistic correction for the oxygen atom has been proposed very recently by Takahashi and Pettersson³³ and is applied in the present work to all theoretical spectra.

Geometrical data of selected model clusters for H_3O^+ and the H_5O_2^+ used for the spectrum calculations are shown in Table I. They were obtained at the Møller-Plesset second-order (MP2) perturbation method level of theory as described in Ref. 34. The aug-cc-pVTZ triple-valence basis set augmented with diffuse basis functions on the oxygen was used in the geometry optimization.

Nonprotonated (“pure”) water is modeled using clusters based on the tetrahedral configuration of ice Ih with the nearest neighbor O–O distance taken to be 2.75 Å as experimentally determined.³⁵ These clusters include up to the second solvation sphere of the excited central water molecule and provide XA spectra in agreement with those from bigger clusters⁸ and periodic calculations.³¹ Although model clusters based on the tetrahedral local structure of ice Ih are not representative of the liquid phase and will result in XA spectra dissimilar to that of water,⁸ they are used here with various distortions around the central unit to compare with the protonated species in the same H-bond configuration.

DFT spectra were computed using the transition-potential approach.^{16,18} In each of the spectrum calculations based on the CPMD structures the excited molecule was placed in the center of a cluster containing 24 water molecules and one proton. The selected configurations were, based on simple geometrical criteria,³⁶ categorized as Eigen (11 structures, 11 excited oxygen atoms) or Zundel species (14 structures, 28 excited oxygen atoms). The spectrum for each of the categories was obtained by summing the individual spectra of all the structures in the category convoluted with Gaussian line profiles of constant full width at half maximum of 0.5 eV.

D. Molecular dynamics simulations

The CPMD simulations³⁰ employed the gradient-corrected exchange-correlation density functional BLYP,^{14,37}

periodic boundary conditions, a plane-wave basis set with a plane-wave cutoff of 70 Ry, and Troullier-Martins norm conserving pseudopotentials.³⁸ The fictitious electronic mass was fairly low, i.e., 400 a.u., which ensured that the properties of the system are reasonably converged with respect to this mass.³⁹ The time step was 0.1 fs. The temperature was kept at 298 K by a Nosé-Hoover thermostat.⁴⁰ The CPMD program⁴¹ was used.

The periodic cubic box contained 32 water molecules and one extra proton. The side lengths of the box were 9.862 Å. The total charge of the unit cell was +1 with a uniform compensating background charge⁴² in the simulations of the solvated proton. Initially a liquid water analytical-potential simulation using a flexible version⁴³ of the MCY potential⁴⁴ was performed. In the last frame the proton was placed near a water molecule that at that instant accepted only one H bond and thus had a free electron pair suitable for accommodating the proton. Then a MD simulation of the proton plus liquid system was run for 12 ps using the proton-transfer water potential OSS2.^{34,45} Subsequently a CPMD simulation was performed during an equilibration period of 5 ps followed by a production period of 4 ps, from which atomic coordinates were extracted at regular intervals. Selected molecular configurations around the center at the hydrated proton complex were then used in the spectrum computations which were performed using the STOBE-DEMON program.

III. RESULTS AND DISCUSSION

The H-bond length in aqueous solutions depends strongly on the charge state of the involved molecule.^{5,34,35,46} In pure water the donating and accepting H bonds of the neutral molecules have on the average the same strength whereas for a negative OH^- species in water the accepting H bonds will be much stronger,⁴⁷ the reverse holds with stronger donating H bonds for a protonated water molecule H_3O^+ with a local positive charge.

It has been demonstrated long ago that the resonance energy in an XA spectrum is sensitive to the local bond length, denoted “bond length with a ruler.”⁴⁸ The postedge resonance at 540–541 eV in the oxygen *K*-edge absorption spectra of water and ice is attributed to the donating H bonds and is due to excitation into antibonding states localized along the H bond.²⁵ Since these states are antibonding not only in terms of the intramolecular OH σ bond but also with respect to the intermolecular H-bond, the energy position of the postedge becomes sensitive to the H-bond distance. This has been demonstrated for water by Odelius *et al.*⁴⁹ and is shown in Fig. 1 to be true also for Zundel and Eigen species, where we systematically vary the donating H-bond distance in the cluster models. We observe that both the Eigen and Zundel forms at the same donating H-bond distance show very similar spectra and that the protonated clusters present a nearly linear upward shift of ~ 0.6 eV in the postedge position for each reduction of 0.1 Å in the donating H-bond distance.

High level *ab initio* calculations³⁴ have demonstrated that the H bonds between the protonated Eigen species and

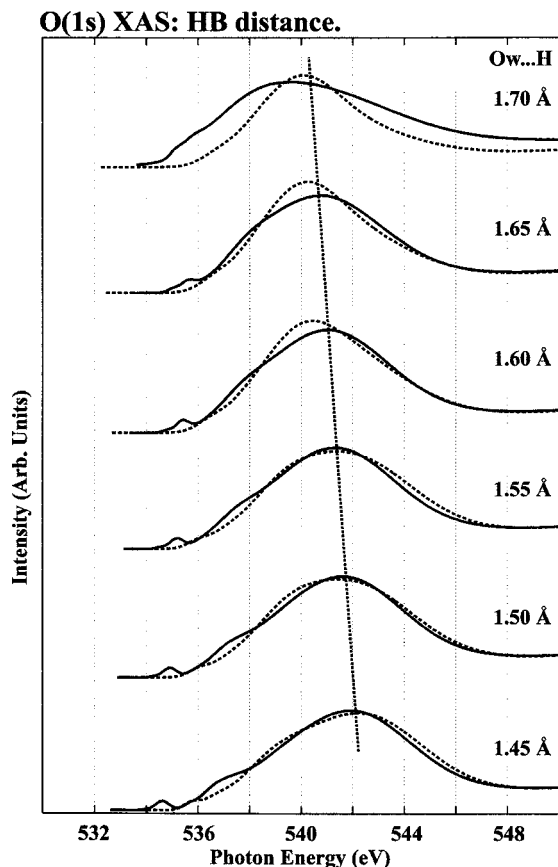


FIG. 1. Computed spectra of the protonated oxygen in the Eigen (solid lines) and Zundel (dotted lines) cations as a function of the donating H-bond distance to neighboring water molecules. The broad conduction band center (postedge peak) shows a downward shift of ~ 0.6 eV with each 0.1 Å H-bond elongation. (The preedge peak is absent due to the double-donor configuration used in the cluster model, c.f. Fig. 5).

its first hydration sphere are substantially shorter than the usual H bonds in bulk water and ice while the hydrated $\text{H}_5\text{O}_2^+(\text{H}_{13}\text{O}_6^+)$ in solution is H bonded at only somewhat shorter distance than bulk water. For a protonated water complex the donating H-bond length will thus be shorter if the proton, as in the Eigen form, is localized on one molecule instead of being shared between two or several molecules as in the Zundel form. Based on this we could thus expect to use changes in the postedge resonance energy in acidic solutions compared to pure water to characterize in more detail the structure of the protonated complex. Note that this interpretation is very different from that of Cappa *et al.*⁵⁰ who have very recently reported on studies of HCl and NaCl solutions and discuss in terms of the change in ionization potential (IP) due to the charge. However, XAS is not an ionization spectroscopy and for the states in the low energy part of the spectrum the difference in electrostatic potential for the electron in the initial $1s$ and excited state has negligible effects. This is clearly shown in Fig. 5 in Ref. 50 where a spread in IP of more than 6 eV leads to no variation in the onset and general shape of the displayed spectra (the particular case of Cl^- will be discussed below). We furthermore note, in contrast to what is stated in Ref. 50, that their 4M NaCl spectrum is at strong variance with their earlier published spectrum of NaCl at a similar concentration,⁵¹ which

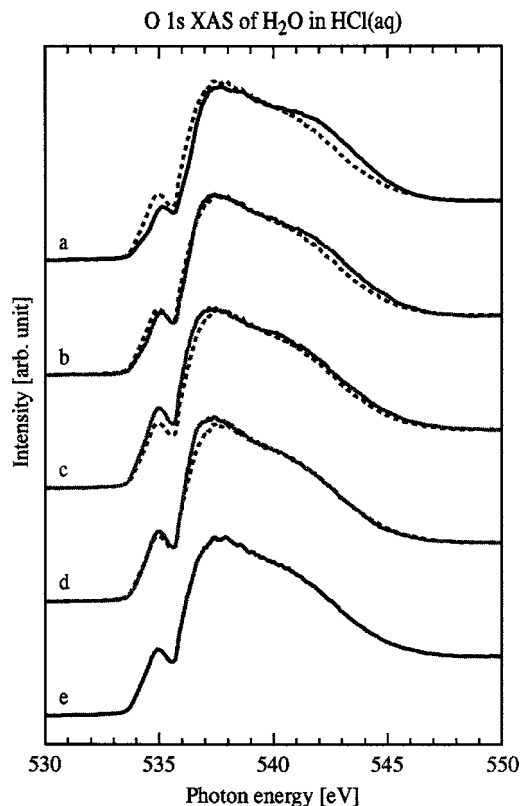


FIG. 2. $\text{O}1s$ XAS of (a) 6M HCl(aq), (b) 4M HCl(aq), (c) 1M HCl(aq), (d) 0.1M HCl(aq), and (e) pure water. The 0.1M HCl(aq) spectrum and the 1M HCl(aq) spectrum show small changes compared to the pure water spectrum (dotted), including an increase of the intensity in the preedge and main-edge regions. These intensities decrease with increasing concentration and the whole spectrum is shifted upward in energy. All spectra are intensity normalized at 550 eV.

is indicative of experimental artifacts due to saturation effects.^{10,52}

The measured oxygen K -edge x-ray absorption spectra of 0.1, 1, 4, and 6M aqueous solutions of HCl are compared in Fig. 2 with the corresponding spectrum of pure water. The spectra are normalized to equal intensity at 550 eV in order to facilitate visual comparison of the contributions from protonated species in the difference spectra in the postedge region. The difference spectra in Fig. 3 enhance the effects due to the solvated ions (Cl^- , H_3O^+ and/or H_5O_2^+). Note that the normalization only affects the base line; with the chosen normalization the differences do not need to integrate to zero.

At low concentration, 0.1 and 1M HCl(aq), the pre- and main-edge peaks increase compared to pure liquid water [compare the difference spectra in Figs. 3(d) and 3(c)] while at high concentration, 4 and 6M HCl(aq), the intensity in the postedge region is increased while the pre- and main-edge regions decrease [Figs. 3(b) and 3(a)]; there thus seem to be at least two processes affecting the H-bond network in acid solution dominant at low and high concentrations, respectively. In addition we observe a shift of the postedge peak from 540 to 541 eV at low concentration (0.1M) to 541–542 eV at high concentration (6M).

The increased pre- and main-edge peaks at low proton concentrations (0.1 and 1M) indicate that, in spite of the enhanced strength of the H bonds in the immediate vicinity

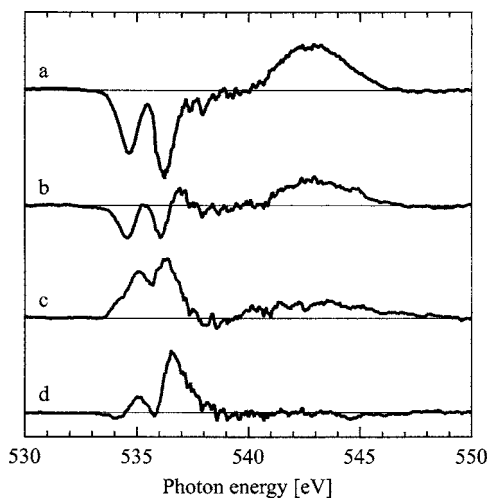


FIG. 3. Difference spectra between the acidic solution XA spectra and the pure water spectrum for (a) 6M HCl(aq), (b) 4M HCl(aq), (c) 1M HCl(aq), and (d) 0.1M HCl(aq). In the 0.1M HCl(aq) spectrum and the 1M HCl(aq) spectrum the positive peaks at 535 and 536.5 eV and the negative peak around 539 eV are indications of an increase of SD configurations (Ref. 8). The loss of intensity around 539 eV is, however, to some extent compensated by the broad feature at 538–550 eV that originates from protonated species. The reverse trend is observed for the higher concentrations.

of the protons, the average number of donating H bonds per molecule is reduced as compared to pure liquid water. The expected decrease in the low energy part of the postedge region (538.5–540 eV) corresponding to the decrease of fully coordinated, double-donor (DD) species is to some extent compensated by an intensity increase in the same energy region originating from species arising upon adding protons.

The spectra of highly concentrated HCl(aq) (4 and 6M), on the other hand, are instead characterized by enhanced intensity in the high energy region around 542–543 eV of the postedge and with an intensity decrease at the preedge. Furthermore, we note a small shift of the preedge peak towards higher energies in comparison with pure water. In Fig. 4 we show the difference spectra in the postedge region for the 1, 4, and 6M HCl(aq) normalized by the proton concentrations, i.e., multiplied by a factor 1, 1/4, and 1/6, respectively. We note that, in this region, the peak shapes and heights of the 4 and 6M difference spectra are very similar, while the 1M difference spectrum is substantially broader and has a peak height that is close to twice as large as for the other two. The close similarity of the 4 and 6M difference spectra after normalization with the proton concentration indicates that similarly bonded species dominate in the 4 and 6M cases, i.e., the number of water molecules affected by a

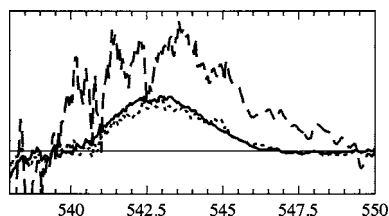


FIG. 4. The region 538–550 eV shown with the 6M (solid), 4M (dotted), and 1M (dashed) difference spectra scaled by a factor 1/6, 1/4, and 1, respectively.

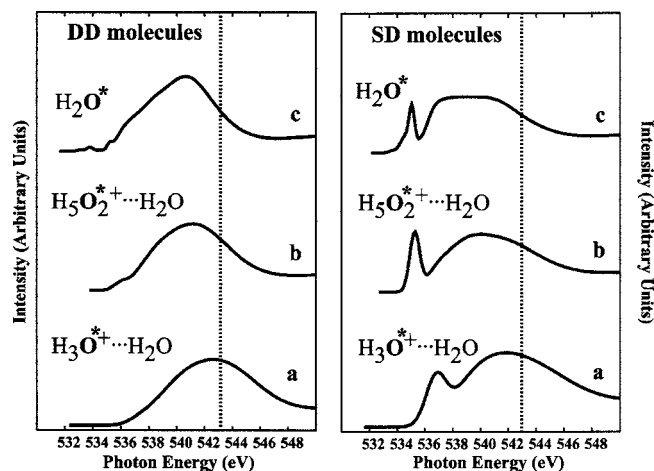


FIG. 5. Computed O1s x-ray absorption spectra of the protonated molecules in (a) the Eigen ($\text{H}_3\text{O}^+\dots\text{H}_2\text{O}$), and (b) Zundel ($\text{H}_5\text{O}_2^+\dots\text{H}_2\text{O}$) cation, and of (c) pure water (H_2O). Configurations in which the excited water molecule is fully coordinated (DD) or with an unsaturated donating hydrogen bond (SD) were considered.

proton scales simply with the proton concentration. From the similarity in shape and the sensitivity to H-bond distance observed in Fig. 1 we furthermore conclude that the structure around the protonated species is similar in the 4 and 6M solutions. The 1M difference spectrum, on the other hand, indicates that for the lower proton concentration more than one oxygen are affected per added proton; this follows from the excess intensity after normalizing by the proton concentration. Furthermore, the larger width of the 1M difference spectrum in the postedge region suggests protonated species that are less well defined in terms of H-bond distances compared to the 4 and 6M cases. Hence, Fig. 4 suggests a larger fraction of distorted Zundel-type species contributing two perturbed oxygens per proton in the case of 1M HCl(aq), while at higher concentration the Eigen form with only one perturbed oxygen per proton dominates. This qualitative change occurs in the interval 1–4M concentration.

We now turn to theory to analyze the observed changes in terms of specific H-bond situations. In particular, the energy shift of the postedge will be used to characterize the structure and bonding of the protonated complexes. The spectra of water molecules in the first solvation sphere of the protonated species in different bonding situations resemble in shape those obtained for the first solvation shell of a water molecule (not shown). Changes with proton concentration are thus due to changes in H bonding and to the presence of protonated water. Both the Eigen and Zundel cationic forms of the excited oxygen directly bonded to the proton are considered in the selected examples of computed spectra in Fig. 5. The structures were taken from a quantum chemical optimization giving H-bond distances of 1.55 and 1.7 Å for the Eigen and Zundel forms, respectively.³⁴ Furthermore, both the Eigen and Zundel species give spectra that are quite similar in intensity for all characteristic features, in the case of both saturated and asymmetric H-bond configurations (DD and SD, respectively, see Fig. 5). However, the spectra for the Eigen and Zundel species differ markedly in energy: the H_3O^+ spectra present an upward shift in the order of 1 eV

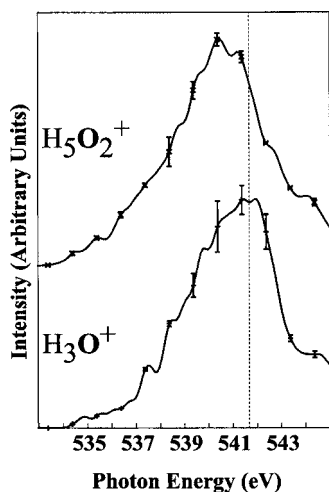


FIG. 6. Summed computed spectra for Eigen (H_3O^+ , 11 structures) and Zundel (H_5O_2^+ , 14 structures, 28 excited oxygens) forms of protonated water using configurations from the CPMD simulation. A constant Gaussian convolution (0.5 eV) is used. The vertical bars in the spectra indicate the standard deviations in the sets of computed spectra in a given point.

compared to H_5O_2^+ and bulk water. This shift occurs for both the postedge and the preedge and is in agreement with the experimental observations in Fig. 2(a) and 2(b). The nature of this shift can be understood in terms of differences in the donating H-bond distances in the two cases, as shown in Fig. 1.

In order to investigate how this carries over to the liquid we have computed the spectra of selected configurations extracted from an *ab initio* CPMD simulation³⁰ of one excess proton in a 32 water molecules simulation box. The spectra in Fig. 6 were computed only for the protonated water molecules and thus only show this specific contribution.

We first note in Fig. 6 that the consistent shift of the postedge peak to higher energy for the H_3O^+ species indicates that the origin of the enhanced intensity at high energy, characteristic of concentrated acid solutions, can be related to the presence of H_3O^+ species, consequently suggested to be the dominant protonated form in solution at high proton concentration. Note that the lack of significant preedge intensity in the spectra is due to the predominance of DD species in the simulation.^{8,49}

The energy shift between the two protonated species in Fig. 6 can be explained by the shorter donating H-bond length of the smaller and more polarizing H_3O^+ cation; in the optimized structures the average donating H-bond distance is considerably longer in the H_5O_2^+ than in the H_3O^+ case (1.7 and 1.55 Å, respectively), which accounts for the shift between the calculated spectra for the two protonated species in Fig. 5. The structures used to obtain the composed spectra in Fig. 6 reflect the same trend with an average H-bond length of 1.55 Å in the Eigen cases and 1.64 Å for the Zundel-type configurations. With the approximate relation of about 0.6 eV energy shift per 0.1 Å H-bond length change the 0.1–0.2 Å H-bond shortening corresponds well with the observed shift of about 1 eV in the postedge peak. The analysis of recent diffraction data by Botti *et al.*⁵ also provides experimental evidence of the very short H bond formed by the H_3O^+ species in concentrated acid solutions, with a resulting

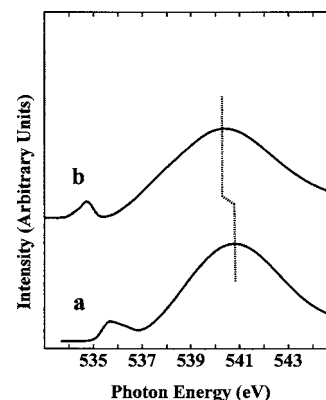


FIG. 7. Simulated spectrum of (a) the protonated Eigen form in the vicinity of the Cl^- counterion and (b) the protonated Zundel cluster in the vicinity of the Cl^- counterion.

average H-bond distance between the protonated species and the neighboring water molecules of 1.50 Å. The broad postedge for the 1M solution, on the other hand, indicates that we have protonated species with a broad distribution of H-bond distances. This could be related to a mixture of Zundel and Eigen forms or fluctuating intermediate structures as proposed by MD simulations.³

The amount of H bonds as defined through the intensity of the pre- and main-edge also undergoes a large change in the range 1–4M HCl(aq). In highly acidic solution the presence of the Eigen species, where the proton is localized on one particular water molecule, leads to strong donating H bonding to the surrounding water molecules. Since the concentration of Eigen species is rather high, nearly all water molecules will be in the first or second solvation shell of the H_3O^+ species resulting in an overall increase in total H bonding. At lower proton concentration the proton is less localized on one particular water molecule and the presence of the solvated ions (Cl^- , $\text{H}_3\text{O}^+/\text{H}_5\text{O}_2^+$) in the solution leads to a reduced number of H bonds compared with pure water.

We note that XAS studies of NaCl and KCl show an increased amount of SD species compared to water in a similar manner as HCl solutions at low concentration.¹¹ The difference spectra for HCl(aq) with concentration up to 1M resemble that of 1M NaCl (or KCl); the only difference being that the enhancement below 536 eV is somewhat larger for 1M KCl while 1M HCl shows a slightly larger enhancement above 542.5 eV. We have investigated the influence of the chloride counterion by explicitly including the Cl^- ion in the theoretical model; in the highly concentrated HCl(aq) solution we can expect one or more Cl^- to be in close vicinity of the protonated cluster as also suggested by both molecular dynamics⁵³ and Monte Carlo⁵ simulations and consistent with diffraction data.

In Fig. 7 we show the computed spectra for the Eigen and Zundel protonated forms in which one Cl^- ion is inserted in the solvation shell of the excited oxygen. The internal O–H distances were taken as 1.01 Å (Eigen form) and 1.0 Å (Zundel form), respectively. As is seen from comparing spectra in Fig. 1 with the spectra in Fig. 7 the coordination to Cl^- does not affect the overall appearance of the spectra. In particular, the significant shift of both postedge and preedge to

higher energy for the Eigen form is preserved also in the case of coordination to chloride. Again this conclusion is very different from that of Cappa *et al.*⁵⁰ who, as in their earlier publication,⁵¹ argue for a charge-induced electronic structure effect on neighboring water molecules due to the Cl^- ion in contrast to the case of Na^+ . This is in spite of the fact that both ions are singly charged and should polarize the environment to a similar extent. The effect of the Cl^- is rather due to the significant difference in H-bond distance, $\sim 3.15 \text{ \AA}$, rather than $\sim 2.75 \text{ \AA}$ as in water. Indeed, computing the XA spectra of water in either SD or DD coordination with one of the H-bonds to a solvated Cl^- or water at 3.15 \AA leads to near-identical spectra.⁵⁴ There is thus no specific effect of the field. The Cl^- simply generates a different and significantly longer H-bond distance when a water molecule coordinates to Cl^- rather than to water.⁵⁴

IV. CONCLUSIONS

XAS shows great sensitivity to the local environment of the hydrated proton and with the aid of DFT-based spectrum calculations it is possible to characterize specific spectral features, in particular, the increasing intensity in the region $>541 \text{ eV}$ in acid solution spectra, as direct signature of the short H bonds formed by the H_3O^+ cation in water. Experimental x-ray absorption spectra of aqueous HCl solutions show different behavior at low and high concentrations of protons. The nonlinear increase in the intensity at higher energy when increasing the concentration of protons suggests a concentration-dependent conversion of the structure of the protonated water from less well-defined Zundel-type (H_5O_2^+) structures to the Eigen (H_3O^+) form. This behavior of highly concentrated acidic solutions is not unexpected based on stoichiometric considerations (the ratio of excess protons per oxygen atom naturally increases with proton concentration) but it is the first time that spectroscopic evidence for a concentration-dependent balance between the two species is obtained. This result reconciles conflicting data where a recent Monte Carlo simulation,⁵ based on neutron diffraction data on highly concentrated HCl solutions, found no evidence for the existence of the H_5O_2^+ cation in seeming contradiction to studies at lower proton concentration.⁴ We find the effects of the proton on the water H-bonding network to be strongly sensitive to the concentration where a high proton concentration reduces the amount of SD species in comparison with pure water while at lower concentrations this is instead increased.

ACKNOWLEDGMENTS

We thank Dr. Tomas K. Hirsch for valuable discussions and help with analyzing the CPMD structures and Dr. Fabio Bruni for making available Monte Carlo simulated structures and radial distribution functions. We acknowledge support from the Basic Energy Sciences (Geosciences, Department of Energy, USA), the Foundation for Strategic Research, the Swedish Royal Academy of Science (KVA), the Göran Gustafsson's Foundation for Research in Natural Science and Medicine, the Swedish Research Council, and the National Science Foundation (U.S.) under Contract Nos. CHE-

0431425 and CHE-0518637. Computer time from the Swedish Center for Parallel Computing (PDC) and the National Supercomputer Center (NSC) is acknowledged. The Advanced Light Source is supported by the Director, Office of Science, Office of Basic Energy Sciences, Material Sciences Division, of the U.S. Department of Energy under Contract No. DE-AC03-76SF00098 at Lawrence Berkeley National Laboratory. Portions of this research were carried out at the Stanford Synchrotron Radiation Laboratory, a national user facility operated by Stanford University on behalf of the U.S. Department of Energy, Office of Basic Energy Sciences.

¹G. Zundel and H. Z. Metzger, *Z. Phys. Chem. (Munich)* **58**, 225 (1968).

²M. Eigen, *Angew. Chem., Int. Ed. Engl.* **3**, 1 (1964).

³D. Marx, M. E. Tuckerman, J. Hutter, and M. Parrinello, *Nature (London)* **397**, 601 (1999); U. W. Schmitt and G. A. Voth, *J. Chem. Phys.* **111**, 9361 (1999); D. Asthagiri, L. R. Pratt, and J. D. Kress, *Proc. Natl. Acad. Sci. U.S.A.* **102**, 6704 (2005); S. Izvekov and G. A. Voth, *J. Chem. Phys.* **123**, 044505 (2005).

⁴J. Kim, U. W. Schmitt, J. A. Gruetzmacher, G. A. Voth, and N. E. Scherer, *J. Chem. Phys.* **116**, 737 (2002).

⁵A. Botti, F. Bruni, S. Imberti, M. A. Ricci, and A. K. Soper, *J. Chem. Phys.* **121**, 7840 (2004).

⁶M. Miyazaki, A. Fujii, T. Ebata, and N. Mikami, *Science* **304**, 1134 (2004); J.-W. Shin, N. I. Hammer, E. G. Diken, M. A. Johnson, R. S. Walters, T. D. Jaeger, M. A. Duncan, R. A. Christie, and K. D. Jordan, *ibid.* **304**, 1137 (2004); J. M. Headrick, J. C. Bopp, and M. A. Johnson, *J. Chem. Phys.* **121**, 11523 (2004); C.-K. Lin, C.-C. Wu, Y.-S. Wang, Y. T. Lee, H.-C. Chang, J.-L. Kuo, and M. L. Klein, *Phys. Chem. Chem. Phys.* **7**, 938 (2005); J. M. Headrick, E. G. Diken, R. S. Walters, N. I. Hammer, R. A. Christie, J. Cui, E. M. Myshakin, M. A. Duncan, M. A. Johnson, and K. D. Jordan, *Science* **308**, 1765 (2005).

⁷S. Myneni, Y. Luo, L. Å. Näslund *et al.*, *J. Phys.: Condens. Matter* **14**, L213 (2002).

⁸Ph. Wernet, D. Nordlund, U. Bergmann *et al.*, *Science* **304**, 995 (2004).

⁹U. Bergmann, Ph. Wernet, P. Glatzel, M. Cavalleri, L. G. M. Pettersson, A. Nilsson, and S. P. Cramer, *Phys. Rev. B* **66**, 092107 (2002).

¹⁰L. Å. Näslund, J. Lüning, Y. Ufuktepe, H. Ogasawara, Ph. Wernet, U. Bergmann, L. G. M. Pettersson, and A. Nilsson, *J. Phys. Chem. B* **109**, 13835 (2005).

¹¹L. Å. Näslund, D. C. Edwards, U. Bergmann, Ph. Wernet, H. Ogasawara, L. G. M. Pettersson, S. Myneni, and A. Nilsson, *J. Phys. Chem. A* **109**, 5995 (2005).

¹²J. Stöhr, *NEXAFS Spectroscopy* (Springer-Verlag, Berlin, 1992).

¹³K. Hermann, L. G. M. Pettersson, M. E. Casida *et al.*, STOBE Software, 2005.

¹⁴A. D. Becke, *Phys. Rev. A* **38**, 3098 (1988).

¹⁵J. P. Perdew, *Phys. Rev. B* **34**, 7406 (1986).

¹⁶J. C. Slater, *Adv. Quantum Chem.* **6**, 1 (1972).

¹⁷J. C. Slater and K. H. Johnson, *Phys. Rev. B* **5**, 844 (1972).

¹⁸L. Triguero, L. G. M. Pettersson, and H. Ågren, *Phys. Rev. B* **58**, 8097 (1998).

¹⁹M. Cavalleri, D. Nordlund, M. Odelius, A. Nilsson, and L. G. M. Pettersson, *Phys. Chem. Chem. Phys.* **7**, 2854 (2005).

²⁰B. Hetényi, F. De Angelis, P. Gianozzi, and R. Car, *J. Chem. Phys.* **120**, 8632 (2004).

²¹W. Kutzelnigg, U. Fleischer, and M. Schindler, *NMR-Basic Principles and Progress* (Springer, Heidelberg, 1990).

²²L. G. M. Pettersson, U. Wahlgren, and O. Gropen, *J. Chem. Phys.* **86**, 2176 (1987).

²³S. Huzinaga, *J. Chem. Phys.* **42**, 1293 (1965).

²⁴H. Ågren, V. Carravetta, O. Vahtras, and L. G. M. Pettersson, *Theor. Chem. Acc.* **97**, 14 (1997).

²⁵M. Cavalleri, H. Ogasawara, L. G. M. Pettersson, and A. Nilsson, *Chem. Phys. Lett.* **364**, 363 (2002).

²⁶M. Cavalleri, D. Nordlund, M. Odelius, A. Nilsson, and L. G. M. Pettersson, *Phys. Chem. Chem. Phys.* **7**, 2854 (2005).

²⁷C. Kolczewski, R. Püttner, O. Plashkevych *et al.*, *J. Chem. Phys.* **115**, 6426 (2001).

²⁸M. Nyberg, M. Odelius, A. Nilsson, and L. G. M. Pettersson, *J. Chem. Phys.* **119**, 12577 (2003).

- ²⁹ K. R. Wilson, B. S. Rude, R. D. Schaller, T. Catalano, R. J. Saykally, M. Cavalleri, A. Nilsson, and L. G. M. Pettersson, *J. Phys. Chem. B* **109**, 10194 (2005).
- ³⁰ R. Car and M. Parrinello, *Phys. Rev. Lett.* **55**, 2471 (1985).
- ³¹ M. Cavalleri, M. Odelius, A. Nilsson, and L. G. M. Pettersson, *J. Chem. Phys.* **121**, 10065 (2004).
- ³² L. Triguero, O. Plashkevych, L. G. M. Pettersson, and H. Ågren, *J. Electron Spectrosc. Relat. Phenom.* **104**, 215 (1999).
- ³³ O. Takahashi and L. G. M. Pettersson, *J. Chem. Phys.* **121**, 10339 (2004).
- ³⁴ L. Ojamäe, I. Shavitt, and S. J. Singer, *J. Chem. Phys.* **109**, 5547 (1998).
- ³⁵ A. K. Soper, *Chem. Phys.* **258**, 121 (2000).
- ³⁶ Eigenspecies are characterized by having three internal O–H bonds under 1.1 Å. In the Zundel configuration the excess proton is shared by two water molecules at maximum water···H+ distance of 1.5 Å.
- ³⁷ C. Lee, W. Yang, and R. G. Parr, *Phys. Rev. B* **37**, 785 (1988).
- ³⁸ N. Troullier and J. L. Martins, *Phys. Rev. B* **43**, 1993 (1991).
- ³⁹ S. Izvekov and G. A. Voth, *J. Chem. Phys.* **123**, 044505 (2005).
- ⁴⁰ S. Nose, *J. Chem. Phys.* **81**, 511 (1984); *Mol. Phys.* **52**, 255 (1984); W. G. Hoover, *Phys. Rev. A* **31**, 1695 (1985).
- ⁴¹ CPMD, version 3.7.2, Copyright IBM Corp. 1990–2003, Copyright MPI für Festkörperforschung Stuttgart 1997–2001; J. Hutter and M. Iannuzzi, *Z. Kristallogr.* **220**, 549 (2005).
- ⁴² M. Tuckerman, K. Laasonen, M. Sprik, and M. Parrinello, *J. Chem. Phys.* **103**, 150 (1995).
- ⁴³ L. Ojamäe, J. Tegenfeldt, J. Lindgren, and K. Hermansson, *Chem. Phys. Lett.* **195**, 97 (1992); M. Wojcik, K. Hermansson, J. Lindgren, and L. Ojamäe, *Chem. Phys.* **171**, 189 (1993).
- ⁴⁴ O. Matsuoka, E. Clementi, and M. Yoshimine, *J. Chem. Phys.* **64**, 1531 (1976).
- ⁴⁵ S. McDonald, S. J. Singer, and L. Ojamäe, *J. Chem. Phys.* **112**, 710 (2000).
- ⁴⁶ S. Imberti, A. Botti, F. Bruni, G. Cappa, M. A. Ricci, and A. K. Soper, *J. Chem. Phys.* **122**, 194509 (2005); T. Head-Gordon and G. Hura, *Chem. Rev. (Washington, D.C.)* **102**, 2651 (2002); A. L. Sobolewski and W. Domcke, *Phys. Chem. Chem. Phys.* **4**, 4 (2002); *J. Phys. Chem. A* **106**, 4185 (2002).
- ⁴⁷ H.-K. Nienhuys, A. J. Lock, R. A. Van Santen, and H. J. Bakker, *J. Chem. Phys.* **117**, 8021 (2002).
- ⁴⁸ J. Stöhr, F. Sette, and A. L. Johnson, *Phys. Rev. Lett.* **53**, 1684 (1984).
- ⁴⁹ M. Odelius, M. Cavalleri, A. Nilsson, and L. G. M. Pettersson, *Phys. Rev. B* **73**, 024205 (2006).
- ⁵⁰ C. D. Cappa, J. D. Smith, B. M. Messer, R. C. Cohen, and R. J. Saykally, *J. Phys. Chem. B* **110**, 1166 (2006).
- ⁵¹ C. D. Cappa, J. D. Smith, K. R. Wilson, B. M. Messer, M. K. Gilles, R. C. Cohen, and R. J. Saykally, *J. Phys. Chem. B* **109**, 7046 (2005).
- ⁵² A. Nilsson, Ph. Wernet, D. Nordlund *et al.*, *Science* **308**, 793a (2005).
- ⁵³ A. J. Sillanpää, and K. Laasonen, *Phys. Chem. Chem. Phys.* **6**, 555 (2004).
- ⁵⁴ L. Å. Näslund, H. Ogasawara, M. Odelius, L. G. M. Pettersson, and A. Nilsson (unpublished).